

Reversible electron transfer in photochemistry and electrochemistry

A. I. Burshtein^{a)} and A. A. Neufeld

Department of Chemical Physics, Weizmann Institute of Science, 76100 Rehovot, Israel

K. L. Ivanov

International Tomography Center, 630090 Novosibirsk, Russia

-Received 22 February 2001; accepted 18 May 2001!

A complete set of integral equations is used to describe the kinetics of reversible photoionization after instantaneous excitation, including geminate and bimolecular charge recombination, to either the ground or excited states of neutral products. The normalized distribution of ionization products, calculated taking into account reverse electron transfer, differs from that for irreversible photoionization. At low reorganization energy and slow diffusion, the reversibility of the quasiresonant ionization reduces its quantum yield, but does not affect the charge separation quantum yield. The excitations restored by bimolecular recombination of ions produce the delayed fluorescence which goes to zero as a second power of time. The quantum yield of the electroluminescence detected after injection of ions into solution has a sharp free energy dependence, like that observed experimentally. © 2001 American Institute of Physics.

@DOI: 10.1063/1.1385161#

I. INTRODUCTION

The vast majority of works which study the impurity ionization of excited molecules are confined to highly exergonic electron transfer. Under such conditions the reverse electron transfer regenerating the excited state can be forgotten. All photogenerated ions recombine uniquely into the ground state of the neutral products. An important exception to this rule was demonstrated in a pioneering work of Rehm and Weller.¹ They studied the Stern–Volmer ionization constant as a function of the free energy of transfer at the contact distance s , $DG_i = DG_i(s)$. This experimental study covers a wide range of free energies including positive values of this quantity, wherein the rate of reverse transfer to the excited state, $W_B(r)$, is not negligible. In fact, at $DG_i > 0$ it is even larger than the forward one, $W_I(r)$, since they are related to each other via the detailed balance principle,

$$W_B \cdot r = W_I \cdot r \exp(DG_i / T). \quad -1.1!$$

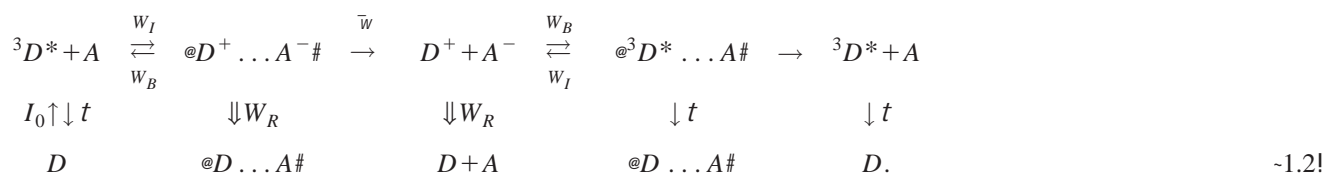
Here and below the Boltzmann constant $k_B = 1$, so that T is the absolute temperature, measured in units of energy ($1 \text{ eV} \approx 1.16 \times 10^4 \text{ K}$). In the Rehm–Weller work the reversibility of ionization was accounted for by means of elementary Markovian chemical kinetics, assuming that all the reaction constants are time independent. The initial nonstationary development of the process was later taken into account, but only for irreversible ionization.^{2,3} This was done in the framework of non-Markovian differential en-

counter theory,^{4,5} which is of no use when the reversibility of photoionization is an essential part of the phenomenon.

The more general integral encounter theory -IET! derived from first principles⁶ was first applied to reversible ionization only recently.⁷ IET is perfect for highly diluted solutions, but for higher reactant concentration its modified version should be better used.^{8,9} Unlike their differential analogs, integral theories were recently recognized as a universal approach to reversible bimolecular reactions of metastable particles.^{7,10–12}

In the present article IET is applied to photoionization resulting in accumulation and separation of counterions. Their subsequent bimolecular recombination in the bulk restores the excited state population. The latter is responsible for the delayed fluorescence, lasting longer than the initial decay of excitation with lifetime t . A similar effect was obtained by injecting a large number of ions into solution and detecting the fluorescence produced by their recombination.^{13–17}

In Ref. 17 both fluorescence quenching and electroluminescence were studied. The excited triplet state of tris-2,2'-bipyridine!ruthenium-II! complex ${}^3\text{Ru}(\text{bpy})_3^{2+}$ was used as an electron donor, ${}^3D^*$, and quinone or some radicals were electron acceptors, A . The triplet quenching after photoexcitation, followed by radical ion separation and recombination to either the excited or ground state of D is represented by the following reaction scheme:



^{a)} Author to whom all correspondence should be addressed.

Electronic mail: anatoly.burshtein@weizmann.ac.il

The excitation of triplets by charge recombination is also possible when ions are produced from the singlet excited state.¹⁸ However, the participation of both singlet and triplet donor states in electron transfer makes the reaction scheme more complex and we shall defer such a generalization until a later time.

The left half of reaction scheme -1.2! describes reversible photoionization and separation of those ions which escape geminate recombination. This part of the reaction is usually the subject of a picosecond study of charge separation whose quantum yield \bar{w} is a source of information about the recombination rate.¹⁹ The right half of the same scheme is related to the further evolution of the free ions which recombine in binary encounters, either to the ground state or back to the excited donor state. The latter is responsible for a delayed fluorescence which occurs with a characteristic time of bimolecular charge recombination. The whole scheme allows one to consider jointly both short time geminate and long time bimolecular recombination, as well as the total quantum yield of stationary fluorescence.⁷

In Sec. II we will present the closed set of IET equations which constitute the formal basis for the kinetic description of the whole multistage reaction. In Sec. III the short time evolution of the system -geminate stage! is described with special attention paid to the distribution of charge products and the quantum yield of reversible ionization. In Sec. IV we analyze the long time asymptotic behavior and the free energy dependence of delayed fluorescence. In Sec. V we calculate the free energy dependence of the electroluminescence quantum yield in the contact approximation and account for the space dispersion of transfer rates, essential for diffusional effects. It is shown that ionization, which is reverse transfer regarding recombination to the excited state, cannot be ignored here especially in nonpolar solutions. All calculations are performed with an original program that allows us to solve numerically integral equations and reproduce the whole kinetics of energy dissipation and ion relaxation. In conclusion, we emphasize once again the advantages of the integral theory in solving all kinetic problems of photochemistry and electrochemistry regardless of their complexity.

II. REVERSIBLE IONIZATION FOLLOWED BY RADICAL ION RECOMBINATION

A. General form of IET equations

We restrict our consideration to the particular case when the neutral acceptors are in such a great excess that they are not essentially expended due to ionization. Then their concentration is not changed ($@A\# = c = \text{const}$) and the general equations obtained recently by regular means^{7,12} can be simplified to the following set:

$$\begin{aligned} \dot{N}^*-t! &= -c \int_0^t R^*-t!N^*-t-t!dt \\ &+ \int_0^t R^\#-t!@N^+-t-t!\#^2dt - \frac{N^*-t!}{t} + I_0-t!N, \end{aligned} \tag{2.1a}$$

$$\begin{aligned} \dot{N}^+-t! &= c \int_0^t R^\dagger-t!N^*-t-t!dt \\ &- \int_0^t R^\ddagger-t!@N^+-t-t!\#^2dt. \end{aligned} \tag{2.1b}$$

Here N^* is the density of the excited molecules while $N^+ = @D^+\# = @A^-\#$ is the total concentration of radical ions in solution, in pairs and in the bulk. The equations include light pumping with rate I_0 and the excited state decay with time t . It is also assumed that the light pumping is too weak to affect the kernels of integral equations as it does at higher light power.²⁰ Even more so, the pumping is so weak that it does not exhaust the ground state whose population N remains the same -equilibrium! all the time.

The kernels R^* and R^\dagger , given by their Laplace transformations $\tilde{R}(s) = \int_0^\infty R(t)e^{-st} dt$, are different:

$$\tilde{R}^*-s! = \left(s + \frac{1}{t}\right) \int @W_I-r!\tilde{n}-r;s! - W_B-r!\tilde{m}-r;s!\#d^3r, \tag{2.2a}$$

$$\begin{aligned} \tilde{R}^\dagger-s! &= \left(s + \frac{1}{t}\right) \int @W_I-r!\tilde{n}-r;s! - W_B-r!\tilde{m}-r;s! \\ &- W_R-r!\tilde{m}-r;s!\#d^3r. \end{aligned} \tag{2.2b}$$

The former accounts for only reversible ionization, with the forward and reverse transfer rates, $W_I(r)$ and $W_B(r)$, while the latter in addition accounts for irreversible recombination to the ground state with a rate $W_R(r)$. Both kernels are expressed via the Laplace transformation of pair correlation functions n and m . They obey the auxiliary equations:

$$\left[s + \frac{1}{t} + W_I + \mathcal{L}_r\right] \tilde{n}-r;s! - W_B\tilde{m}-r;s! = 1, \tag{2.3a}$$

$$@s + W_B + W_R + \mathcal{L}_r^\# \tilde{m}-r;s! - W_I\tilde{n}-r;s! = 0, \tag{2.3b}$$

with reflecting boundary conditions at the distance of closest approach $r = S$. The linear operators

$$\mathcal{L}_r = \frac{1}{r^2} \int r^2 D-r! \frac{J}{J_r}, \tag{2.4a}$$

$$\mathcal{L}_r^\# = \frac{1}{r^2} \int r^2 \tilde{D}-r! \left[\frac{J}{J_r} + \frac{1}{T} \frac{dU-r!}{dr} \right], \tag{2.4b}$$

define the relative diffusive motion of neutral reactants and ions, respectively, with the corresponding diffusion coefficients D and \tilde{D} that may be different and distance dependent. The diffusional operator for ions also differs from those for neutral reactants. It accounts for the Coulomb attraction within a well of Onsager radius r_c , which is represented by the electrostatic potential $U(r)$.

The Laplace transformations of the kernels, representing the bimolecular recombination to the ground and excited states, are

$$\begin{aligned} \bar{R}^{\ddagger}_{-s} = & s \int @W_{R-r} \tilde{f}_{-r}; s! + W_{B-r} \tilde{f}_{-r}; s! \\ & - W_{I-r} \tilde{g}_{-r}; s! \# d^3 r, \end{aligned} \quad -2.5a!$$

$$\bar{R}^{\#}_{-s} = s \int @W_{B-r} \tilde{f}_{-r}; s! - W_{I-r} \tilde{g}_{-r}; s! \# d^3 r, \quad -2.5b!$$

where the auxiliary pair distributions obey the following set of equations:

$$\left[s + \frac{1}{\bar{t}} + W_I + \mathcal{L}_r \right] \tilde{g}_{-r}; s! - W_B \tilde{f}_{-r}; s! = 0, \quad -2.6a!$$

$$@s + W_B + W_R + \mathcal{L}_r^c \tilde{f}_{-r}; s! - W_I \tilde{g}_{-r}; s! = 1. \quad -2.6b!$$

For particular calculations, based on the IET equations, we need information about spatial shape and the strength of the reaction rates $W_{I,B,R}$ which depend on several parameters, e.g., reaction exergonicities, reorganization energies, preexponential factors, and the length of tunneling.

B. Spatial dispersion of reaction rates

As can be seen, the input data for the theory are the kinematic parameters (D , \bar{D} , r_c , and S) and distance dependent rates of remote electron transfer between reactants. Deduced using the “golden rule” of conventional perturbation theory¹⁹ all of them have the same general shape conforming to the Marcus free energy gap -FEG! law:

$$W_{-r}! = w \sqrt{\frac{1_c}{1-r!}} e^{-2(r-s)/L} \exp\left[-\frac{@DG_{-r}! + 1-r! \#^2}{4 1-r! T}\right], \quad -2.7!$$

where the pre-exponential factor

$$w = \frac{\sqrt{\rho} V_0^2}{\sqrt{1_c T}}. \quad -2.8!$$

Here V_0 and L are matrix elements and the space decrement of electron tunneling, whereas

$$1-r! = 1_i + 1_0 \left(2 - \frac{S}{r}\right) \quad -2.9!$$

is the distance dependent reorganization energy of electron transfer, composed from the intramolecular (1_i) and “outer-sphere” contribution from the continuum media.

All the rates crucially depend on the free energy of ionization,

$$DG_{I-r}! = DG_i + T \left(\frac{r_c}{S} - \frac{r_c}{r} \right). \quad -2.10!$$

Although there are three free energies, only one of them is actually independent, let's say, DG_I . The rest can be expressed through it, because

$$DG_{B-r}! = -DG_{I-r}!,$$

while the sum of the ionization and recombination free energies is fixed by a value of the excitation energy \mathcal{E} of ${}^3D^*$, see Fig. 1,

$$-DG_{I-r}! - DG_{R-r}! = \mathcal{E}. \quad -2.11!$$

When the ionization is highly exergonic and therefore irreversible (

$$h = \frac{N_s^* - c}{N_s^* - c = 0} = \frac{1}{1 + ckt}, \quad -3.5!$$

where N_s^* is the stationary solution of Eq. -2.1! at $I_0 = \text{const}$. This is the true Stern–Volmer relationship for stationary quantum yield of fluorescence, whose constant^{12,7}

$$k = k_0 \left[1 - \frac{\bar{R}^\ddagger - 0}{\bar{R}^* - 0} \right]. \quad -3.6!$$

The same result also follows from the dynamic definition of the quantum yield -3.3!, provided $P^*(t)$ is calculated from the net set of Eq. -2.1!, which accounts not only for the geminate but also for the bulk recombination. The true Stern–Volmer constant k differs essentially from k_0 , which is available from the short-range kinetics of energy quenching.

A. Quantum yields of ionization and charge separation

Making the Laplace transformation for Eq. -3.2!, one can find the height of the plateau

$$N^+_{-t} = \lim_{s \rightarrow 0} s \bar{N}^+_{-s} = c \bar{R}^\ddagger - 0 \bar{N}^* - 0 = \frac{c t \bar{R}^\ddagger - 0 N_0^*}{1 + c t \bar{R}^* - 0}. \quad -3.7!$$

an intermediate stage between the geminate and bimolecular stages -Fig. 2!. Hence, the geminate stage ends by creation of a limited number of free ions, constituting this plateau:

$$N^+_{-t} = N_0^* f. \quad -3.1!$$

Here f is the quantum yield of free ions. The whole kinetics of geminate ion accumulation and recombination is described by the reduced equations -2.1!, omitting those terms related to bimolecular recombination:

$$\dot{N}^*_{-t} = -c \int_0^t R^*_{-t} N^*_{-t-t} dt - \frac{N^*_{-t}}{t}, \quad -3.2a!$$

$$\dot{N}^+_{-t} = c \int_0^t R^\ddagger_{-t} N^*_{-t-t} dt. \quad -3.2b!$$

The initial conditions for them are created by instantaneous excitation at $t=0$:

$$N^*_{-0} = N_0^*, \quad N^+_{-0} = 0.$$

From Eq. -3.2! one can find the short-range kinetics, as well as the quantum yields of ionization and charge separation. In particular, one can obtain the survival probability of excitation $P^*(t) = N^*(t)/N_0^*$, which tends toward zero in this time interval provided the bimolecular restoration of excitations is negligible. The measurable quantity $P^*(t)$ can be used to calculate another one,

$$h_0 = \frac{1}{t} \int_0^t P^*_{-t} dt = \frac{\bar{N}^* - 0}{N_0^* t} = \frac{1}{1 + c k_0 t}, \quad -3.3!$$

which enables finding the quenching constant

$$k_0 = \bar{R}^* - 0, \quad -3.4!$$

if t is known. However, h_0 should not be confused with the true quantum yield of stationary fluorescence

As follows from comparison of Eqs. -3.1! and -3.7!, the free ion quantum yield is

$$f = c_0 \bar{w}, \quad -3.8!$$

where c_0 is the quantum yield of bimolecular ionization and \bar{w} is the charge separation quantum yield:

$$c_0 = \frac{c k_0 t}{1 + c k_0 t} = 1 - h_0, \quad \bar{w} = \frac{\bar{R}^\ddagger - 0}{\bar{R}^* - 0}. \quad -3.9!$$

The general solution of Eq. -2.3b!,

$$\tilde{m}_{-r;s} = \int \tilde{G}_{-r,r_0;s} W_{I-r_0} \tilde{n}_{-r_0;s} d^3 r_0, \quad -3.10!$$

is expressed through the Green function, whose Laplace transformation obeys the following equation:

$$s + W_B + W_R + \mathcal{L}_{r^\#}^c \tilde{G}_{-r,r_0;s} = \frac{d-r-r_0}{4\pi r r_0}. \quad -3.11!$$

Although this equation involves the rate W_B of backward electron transfer, electron transfer (electron transfer) obeys the

rr

Here

$$W_{a-r_0} = 1 - \int W_{B-r} \tilde{G}_{-r, r_0; 0} d^3r \quad -3.15!$$

is the quantum yield of particles which start from distance r_0 and are separated or irreversibly recombine to the ground state. In other words, this is the probability of avoiding reverse electron transfer into the excited state for ions initially separated by distance r_0 . In Eq. -3.14! this quantity is averaged over the normalized initial distribution of interion distances in photogenerated pairs. In IET this distribution is given the following definition:²²

$$f_{-r_0} = \frac{W_{I-r_0} \tilde{n}_{-r_0; 0}}{* W_{I-r} \tilde{n}_{-r; 0} d^3r}. \quad -3.16!$$

If ionization is irreversible ($W_B = 0$), then $\bar{w}_a [1$ and $k_0 [Q$ is the production rate of radical ion pairs -RIPs! which can only recombine to the ground state or separate. In contrast, in the case of reversible ionization ($W_B \neq 0$) there is a fraction of RIPs subjected to backward electron transfer to the excited state and k_0 is reduced by a multiplier $\bar{w}_a < 1$, which is the averaged quantum yield of irrevocable products of ionization.

The RIP separation quantum yield \bar{w} is expressed in Eq. -3.9! through two kernels. One of them already has been specified in Eq. -3.12!. Another can be represented in the same way using Eqs. -2.2b! and -3.10!:

$$\tilde{R}^{\dagger-0} = Q \bar{w}_b, \quad -3.17!$$

where

$$\bar{w}_b = \int W_{b-r_0} f_{-r_0} d^3r_0 \quad -3.18!$$

and

$$W_{b-r_0} = 1 - \int @W_{R-r} + W_{B-r} \# \tilde{G}_{-r, r_0; 0} d^3r. \quad -3.19!$$

Substituting Eqs. -3.18! and -3.12! into Eq. -3.9! we can express the RIP separation quantum yield as the ratio of two others:

$$\bar{w} = \frac{\bar{w}_b}{W_a}. \quad -3.20!$$

When the ionization is irreversible, $\bar{w}_a = 1$, the charge separation quantum yield is equal to \bar{w}_b , which is the share of RIPs which escaped geminate recombination. On the other hand, when the reverse electron transfer into the excited state cannot be neglected, this is only a fraction of the ions which became free after primary ionization. Since ionization is repeated a number of times after restoration of the excited state by reverse transfer, each time a new portion of free ions and neutral products of recombination will be added to the previous ones. Therefore, the total charge separation quantum yield is given by the ratio of \bar{w}_b to \bar{w}_a , which is the fraction of free ions from all irrevocable products of forward electron transfer. To clarify this point let us illustrate it by an example of contact electron transfer.

B. Charge separation quantum yield in contact approximation

Assuming that all transfer reactions occur at contact distance S , we should set

$$W_{-r} = k \frac{d-r-S!}{4\rho r S},$$

where

$$k = \int W_{-r} d^3r. \quad -3.21!$$

The different contact constants will be labeled by corresponding lower case subscripts:

$$k_i = \int W_{I-r} d^3r, \quad k_b = \int W_{B-r} d^3r, \quad -3.22!$$

$$k_r = \int W_{R-r} d^3r.$$

Obviously, the RIP distribution -3.16! in the contact approximation has the trivial form:

$$f_{-r_0} = \frac{d-r_0-S!}{4\rho r_0 S}. \quad -3.23!$$

As follows from the equation pairs -3.14!, -3.15! and -3.18!, -3.19! the contact quantum yields,

$$\bar{w}_a = W_{a-S} = 1 - k_b \tilde{G}_{-S, S; 0}, \quad -3.24!$$

$$\bar{w}_b = W_{b-S} = 1 - k_b + k_r \tilde{G}_{-S, S; 0},$$

are expressed via the single Green function $\tilde{G}(S, S; 0)$. This is the contact value of a more general Green function, that can be found from the integral representation of Eq. -3.11!:

$$\begin{aligned} \tilde{G}_{-r, r_0; s} &= \tilde{G}_{0-r, r_0; s} - \int \tilde{G}_{0-r, r'; s} \\ &\quad \times @W_{B-r'} + W_{R-r'} \# \tilde{G}_{-r', r_0; s} d^3r'. \end{aligned} \quad -3.25!$$

Here $\tilde{G}_0(r, r_0; s)$ is the Green function of nonreacting ions obeying a simpler equation:

$$@_s + \mathcal{L}_r \# \tilde{G}_{0-r, r_0; s} = \frac{d-r-r_0!}{4\rho r r_0}. \quad -3.26!$$

Using the contact rates -3.21! in Eq. -3.25!, we transform it into an algebraic equation leading to the following relationship between the contact Green functions:

$$\tilde{G}_{-S, S; s} = \frac{\tilde{G}_{0-S, S; s}}{1 + @k_b + k_r \# \tilde{G}_{0-S, S; s}}. \quad -3.27!$$

For ions, freely diffusing in highly polar solvents ($r_c \rightarrow 0$), the Green function is well known:²³

$$\tilde{G}_0^{-1} S, S; s! = \frac{1}{k_D} \cdot \frac{1}{1 + \sqrt{s} t_d} \quad -3.28!$$

Here $k_D = 4\rho S\tilde{D}$ is the diffusional rate constant and $t_d = S^2/\tilde{D}$ is the encounter time.

Using these results it is easy to estimate all the quantum yields:

$$\bar{w}_a = \frac{k_D + k_r}{k_D + k_r + k_b}, \quad \bar{w}_b = \frac{k_D}{k_D + k_r + k_b} \quad -3.29!$$

including the main one, first obtained in Ref. 11:

$$\bar{w} = \bar{w}_b / \bar{w}_a = \frac{1}{1 + k_r/k_D} \quad -3.30!$$

In the same work the contact values of $h_0 = 1 - C_0$ were expressed through the constant

$$k_0 = \frac{K_{irr}}{1 + \frac{K_{irr}}{K - k_D + k_r!}} \quad -3.31!$$

where K is the equilibrium constant of reversible electron transfer,

$$K = \frac{k_i}{k_b} e^{-DG_i/T} \quad -3.32!$$

and k_{irr} is the genuine Stern–Volmer constant of irreversible energy quenching:²⁴

$$k_{irr} = \frac{k_i}{1 + \frac{k_i/k_D}{1 + \sqrt{t_d/t}}} \quad -3.33!$$

Unlike k_0 the true constant of stationary fluorescence, calculated in a recently published work,⁷ turns to zero as $k_r \rightarrow 0$:

$$k = \frac{k_{irr}}{1 + k_{irr}/Kk_r!} \quad -3.34!$$

If there is no recombination to the ground state, then all generated ions earlier or later recombine through reverse transfer to the excited state. Therefore, all of them contribute to stationary fluorescence whose quantum yield becomes 1 and $k=0$. Such dramatic changes do not happen to k_0 , which remains finite even at $k_r=0$. Over a short time range after instantaneous excitation, the electron transfer produces temporary quenching which looks irreversible with a quantum yield $h_0 < 1$. Calculating this quantity through $P^*(t)$ one cuts off the delayed fluorescence that will be discussed separately in Sec. IV. In fact, the initial energy quenching not only looks irreversible, but also its quenching constant k_0 only slightly differs from k_{irr} in a limited range of free energies. The correction factor in the denominator of Eq. -3.31! is small for large exergonicity diffusion controlled transfer:

$$\frac{k_{irr}}{K - k_D + k_r!} < \frac{k_D - 1 + \sqrt{t_d/t!}}{k_D + k_r} e^{DG_i/T} \rightarrow 0 \quad \text{at } DG_i \ll -T,$$

but under kinetic control, at $DG_i > |c| \gg T$ it is also small:

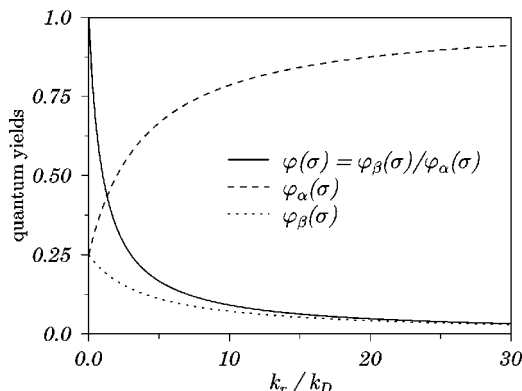


FIG. 3. The partial quantum yields \bar{w}_a -dashed line! and \bar{w}_b -dotted line! in the contact approximation and their ratio \bar{w} -solid line! as functions of the recombination rate constant $k_r, k_b/k_D=3$.

$$\frac{k_{irr}}{K - k_D + k_r!}, \frac{k_i \exp -DG_i/T!}{K - k_D + k_r!}; e^{-(DG_i - 1/c)^2/4|cT}.$$

Hence, the difference between k_0 and k_{irr} -see Fig. 2 in Ref. 11! is confined to the interval:

$$0 < DG_i < |c|. \quad -3.35!$$

The smaller $|c|$ is, the more pronounced is the maximal effect expected in the middle of this interval. The same is true regarding C_0 or h_0 . To emphasize the difference caused by reverse transfer one should choose a donor–acceptor pair with rather small $|c|$.

More significant changes occur with \bar{w}_b and \bar{w}_a . From Fig. 3 we see how the reverse transfer to the excited state reduces \bar{w}_b regarding \bar{w} , and how small \bar{w}_a is regarding the value 1, which it has in the case of irreversible transfer. However, the ratio of these quantities -3.30! remains unchanged at any rate of reverse transfer. This ratio is actually a fraction of the free ions from the total amount of RIPs produced by reversible ionization. The RIPs subjected to reverse electron transfer to the excited state do not contribute to the partial yields estimated in Eq. -3.29!. Each portion of photogenerated RIPs adds some free ions to those in the bulk and partially restores the excitations, generating the next portion of RIPs later on. This cycle is repeated many times until excitations completely vanish. Each time, exactly the same fraction of irrevocable ionization products escape recombination. This fraction being permanent for each portion of photogenerated RIPs remains the same for all of them. Therefore in the contact approximation \bar{w} does not depend on reverse transfer at all.

Extracted from \bar{w} , the free energy dependence of k_r should follow the bell-shaped curve predicted by the Marcus FEG law for the kinetic rate constant. However, this may be just an imitation if recombination is controlled by diffusion from the place where ions were born to their recombination zone.^{19,25} This effect is absent in contact approximation provided the RIPs not only die but are also born at contact. The diffusional distortion of the parabolic FEG law appears only

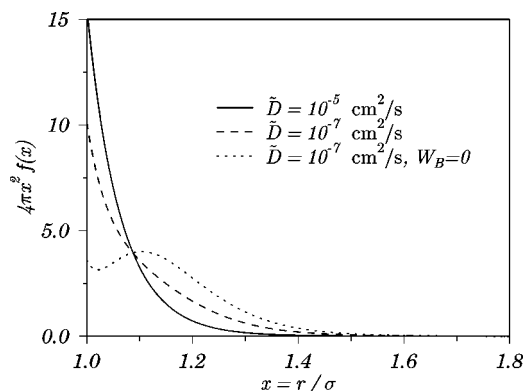


FIG. 4. The effective distributions of ions taking into account reverse transfer -dashed line! and neglecting reverse transfer -dotted line!. Solid line—both of them at faster diffusion -diffusion coefficients are indicated!. The parameters are: $DG_i = -0.1$ eV, $I_c = 0.4$ eV, $w_I = 100$ ns $^{-1}$, $L = 1.4$ Å, $S = 10$ Å, $T = 293$ K, $t = \tau$. The excitation energy of donor \mathcal{E} is assumed to be high, i.e., $W_R = 0$.

in the theory of remote forward and backward electron transfer. The charge separation quantum yield is represented in this theory as

$$\bar{w} = \frac{1}{1 + Z/\bar{D}}. \quad (3.36)$$

The recombination efficiency $Z(DG_r)$ can be affected by encounter diffusion near $-DG_r = \mathcal{E} + DG_i = I_c$, which is close to the top of FEG curve.¹⁹ In Sec. III C we will inspect numerically this curve as well as $k_0(DG_i)$, taking into account the space dispersion of all the rates.

C. Remote reversible ionization

The initial distribution of ions, Eq. (3.16), is determined by the solution of two coupled equations (2.3a), (2.3b), which involve the rates of ionization, recombination, and reverse transfer to the excited state. However, reverse transfer does not affect the shape of the distribution when ionization is under kinetic control, so that $n' \exp(-t/t)$, $m' \approx 0$, and there is nothing to transfer back from m to n . Kinetic ionization creates a distribution identical in form to $W_I(r)$, regardless of the rate of reverse transfer.

Hence, $f(r)$ may be affected only if ionization is under diffusional control. The maximal effect is expected to be at $t = \tau$ when there are stationary functions of distance $n_s(r) = \lim_{s \rightarrow 0} s\tilde{n}(s)$ and $m_s(r) = \lim_{s \rightarrow 0} s\tilde{m}(s)$, with a large dip in $n_s(r)$ near the contact and a hump in $m_s(r)$ at the same place ($n_s + m_s = 1$). The change in product distribution resulting from diffusional distortion of n_s and m_s is demonstrated in Fig. 4 by the example of a system with $t = \tau$, small $I_c = 0.4$ eV and almost resonant ionization ($DG_i = -0.1$ eV). The excitation energy is assumed to be high enough to exclude the recombination of RIPS to the ground state ($W_R = 0$) in this region of ionization exergonicity. To emphasize the effect of reverse transfer, we present calculations in its presence ($W_B = W_I \exp\{DG_i/T\}$) and absence ($W_B = 0$).

At fast diffusion ($\bar{D} = 10^{-5}$ cm 2 /s) the ionization is kinetic controlled and, therefore, there is no visible difference

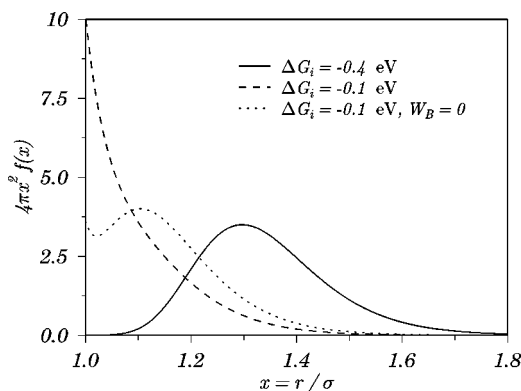


FIG. 5. Initial distributions with and without taking into account the reverse transfer at $DG_i = -0.1$ eV -dashed and dotted lines, respectively! and for $DG_i = -0.4$ eV -solid line, calculation without reverse transfer gives the same curve!. Other parameters are the same as in Fig. 4, except $D = \bar{D} = 10^{-7}$ cm 2 /s for all the curves.

between distributions with and without account for backward transfer. Both of them have the same shape identical to that of $W_I(r)$ -solid line!. At much slower diffusion ($\bar{D} = 10^{-7}$ cm 2 /s), the real initial distribution -long dashed line! even qualitatively differs from that calculated neglecting the reverse process -dotted line!. The latter has a maximum shifted from the contact to the effective reaction radius R_s of diffusion controlled irreversible ionization.²⁶ However, due to reverse transfer and repeated ionization of the excited state there is an accumulation of ionization products near the contact. As a result the form of distribution shown by a long dashed line is qualitatively changed.

The product distribution is subjected to similar changes when DG_i is varied at constant diffusion, see Fig. 5. Since transfer there is controlled by diffusion ($\bar{D} = 10^{-7}$ cm 2 /s), the products of irreversible ionization have a bell-shaped distribution shifted from the contact -solid and dotted line!. The reversible transfer at $DG_i = -0.1$ eV creates another maximum at contact distance -long dashed line!. On the other hand, at higher exergonicity of ionization, $DG_i = -0.4$ eV, the effect of reversible transfer on the effective distribution vanishes and the shape coincides with that for irreversible ionization -solid line!.

Now we can analyze how the reverse transfer affects each quantity in Eq. (3.12). The favorable interval manifests itself by the high but narrow peak in the free energy dependence of Q -solid line on Fig. 6-a!#. This quantity accounts for not only primary, but all subsequent ionization acts followed by reverse electron transfer, which occurs much more often within this interval than outside it. However, for the same reasons the quantum yield of irrevocable forward transfer \bar{w}_a rapidly falls when the free energy approaches the middle of the same interval -Fig. 6-b!#. Therefore, their product $k_0 = Q\bar{w}_a$ does not experience equally dramatic changes, although it vanishes with DG_i faster than in the irreversible case -Fig. 6-c!#. This is an analog of the sharp descent of stationary $k(DG_i)$ found in the same region in Ref. 7. As was expected all these effects are almost eliminated, when I_c is large -long dashed lines in Fig. 6!. Hence, accounting for

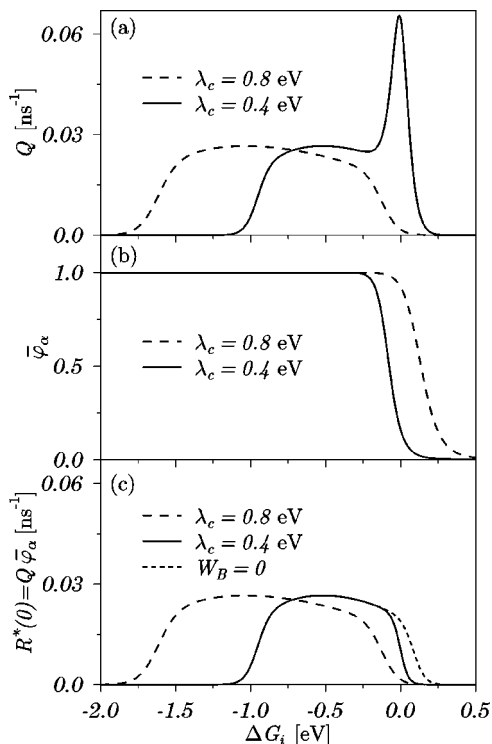


FIG. 6. The effect of transfer reversibility on the free energy dependence of the quenching rate components, Q and \bar{w}_a , as well as on their product $k_0 = \bar{R}^*(0) = Q\bar{w}_a$. Solid lines are for $\lambda_c = 0.4$ eV while dashed lines are for $\lambda_c = 0.8$ eV. The other parameters are the same as for Fig. 5.

the reversibility of electron transfer is important especially for nonpolar solvents, where λ_c is really small. This factor should be more significant for energy transfer which is the fastest under resonant conditions ($DG=0$), where the reversibility is the most pronounced.

As was shown, in the contact approximation the efficiency of charge separation Z is not affected by either diffusion or reverse transfer. Taking into account the space dependence of the transfer rates, the free energy dependence of this quantity can be strongly distorted by diffusion, but the influence of reverse transfer remains negligible (Fig. 7). However, reverse transfer plays a key role in such phenomena as delayed fluorescence and electrochemiluminescence studied in Secs. IV and V.

IV. DELAYED FLUORESCENCE

When geminate recombination is completed and gives way to a bimolecular reaction, the latter restores either excited or ground state neutral products. Since the density of restored states at a late stage of excitation decay is quadratic in concentration of free ions, the latter should be large enough to make the delayed fluorescence detectable. To reach this goal, one should use as strong pumping as possible and choose fluorophors with long lived excited states, then their fluorescence at times $t > \bar{t}$ will be stronger than from natural excitation decay (Fig. 8-a)!

The long-time asymptotics of the delayed decay can be described by the reduced Eqs. (2.1), where the pumping terms are omitted:

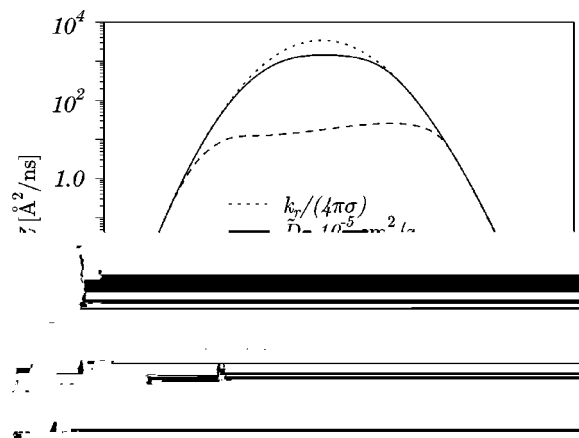


FIG. 7. The free energy dependence of the recombination efficiency parameter Z for fast ($D = \bar{D} = 10^{-5}$ cm²/s, solid line) and slow ($D = \bar{D} = 10^{-7}$ cm²/s, dashed line) diffusion at $\lambda_c = 0.4$ eV and $\epsilon = 1$ eV. The former only slightly differs from $k_r(DG_i)/4\rho S$ (dotted line) peculiar to kinetic controlled geminate recombination. In the latter case $Z(DG_i)$ dependence is strongly distorted by diffusion, but neither of the curves is affected by reverse transfer.

$$\dot{N}^* - t! = -\frac{N^* - t!}{t} - c \int_0^t R^* - t! N^* - t - t! dt + \int_0^t R^\# - t! N^+ - t - t! dt, \tag{4.1a}$$

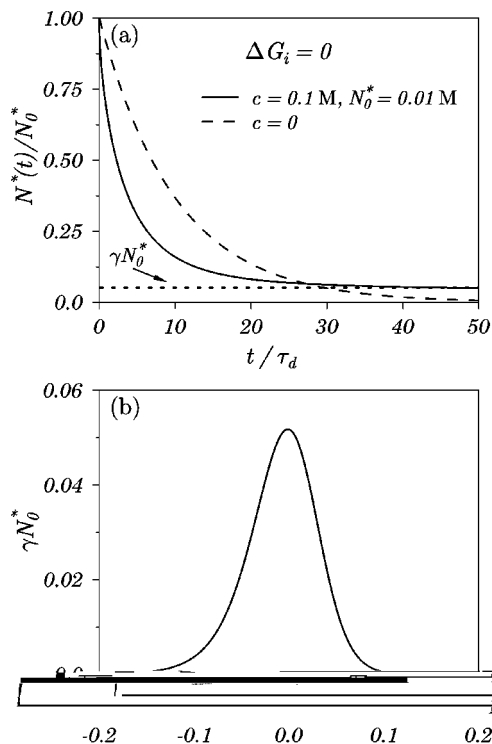


FIG. 8. -a! The kinetics of excitation quenching followed by delayed decay (solid line) in comparison to the free exponential decay (long dashed line). The amplitude of the delayed fluorescence, calculated by Eq. (4.11), is shown by the short dashed line. The initial concentration of the excitations $N_0^* = 0.01$ M, $t = 1$ ms. The other parameters are the same as for Fig. 2. -b! The free energy dependence of the amplitude of delayed decay related to the initial concentration of excitations $N^*(0)/N_0^* = gN_0^*$.

$$\dot{N}^{*-}t = - \int_0^t R^{\ddagger-}t @ N^{*-}t - t! \#^2 dt. \quad -4.1b!$$

The initial condition for free ions prepared by RIPS separation, follows from Eq. -3.1!:

$$N^{*-}0 = N_0^* f = N_0^* c_0 \bar{w}. \quad -4.2!$$

Since ions are stable particles, those terms in integral equations -4.1! which describe ion recombination may be transformed into their differential and even Markovian analogs at $t \gg t_d$.^{21,24} The same can be done with the last ionization term, but at much larger times, $t \gg t$, when concentration of excitations levels off and decreases slowly backing by recombination. Hence, the delayed fluorescence can be described by the following set of differential equations:

$$\dot{N}^{*-}t = k^* @ N^{*-}t \#^2 - \left[\frac{1}{t} + c K_0 \right] N^{*-}t, \quad -4.3a!$$

$$\dot{N}^{*-}t = -k^{\times} @ N^{*-}t \#^2, \quad -4.3b!$$

where $k^* = \bar{R}^{\ddagger}(0)$ and $k^{\times} = \bar{R}^{\ddagger}(0)$. These kernels in the contact approximation are⁷

$$\bar{R}^{\ddagger} = \frac{k_b}{Z}, \quad \bar{R}^{\ddagger-s} = \frac{k_b + k_r + k_i k_r \tilde{g}_1}{Z},$$

where $Z(s) = (1 + k_i \tilde{g}_1(s))(1 + k_r \tilde{g}_2(s)) + k_b \tilde{g}_2(s)$, and

$$\begin{aligned} \tilde{g}_1-s &= @k_D - 1 + \sqrt{s t_d + t_d/t} \#^{-1}, \\ \tilde{g}_2-s &= @k_D - 1 + \sqrt{s t_d} \#^{-1}. \end{aligned} \quad -4.4!$$

Using these results we get the following recombination constant:

$$k^{\times} = \frac{-k_r + k_b' k_D}{-k_r + k_b' + k_D},$$

where $k_r + k_b'$ is its kinetic value. The latter is the sum of recombination rates to the ground state k_r and to the excited one:

$$k_b' = \frac{k_b}{1 + \frac{k_i/k_D}{1 + \sqrt{t_d/t}}}. \quad -4.5!$$

Here exactly the same correction of denominator appeared as in Eq. -3.33!. It accounts for the initial ionization which proceeds nonstationary under diffusional control of electron transfer. As a result an equilibrium relationship between these constants is preserved: $k_{irr}/k_b' = K$.

The solution of Eq. -4.3b! reproduces the usual second-order kinetics:

$$\frac{1}{N^{*-}t} = \frac{1}{N^{*-}0} + k^{\times} t, \quad -4.6!$$

where $N^{*-}(0)$ is specified in Eq. -4.2!. At $t \gg t$ there is the quasistationary solution of Eq. -4.3a!, which yields the following concentration of fluorescent particles:

$$N^{*-}t = k^* t^* @ N^{*-}t \#^2 - t!,$$

where

$$\frac{1}{t^*} = \frac{1}{t} + c K_0. \quad -4.7!$$

Here $N^{+}(t)$ is given by Eq. -4.6! and k_0 by Eqs. -3.31!, -3.32!:

$$k_0 = k_b' K \frac{k_D + k_r}{k_D + k_r + k_b'},$$

where

$$K = \frac{k_i}{k_b}, \quad -4.8!$$

and the effective constant of backward transfer k_b' is defined by Eq. -4.5!. The long-time asymptotic decay of excitation is quadratic in time:

$$N^{*-}t \sim \frac{k^* t^*}{-k^{\times} t^2} = \frac{A}{t^2}, \quad -4.9!$$

where A is estimated in the contact approximation as

$$A_c = t \frac{k_b'}{k_D} \frac{k_D + k_r + k_b'}{-1 + c K_0 t - k_r + k_b'}. \quad -4.10!$$

As far as we know the very fact of experimental registration of delayed fluorescence was not reported yet due to the very rigid conditions for its observation. The number of second time excited molecules does not exceed

$$N^{*-}0 = k^* t^* @ N^{*-}0 \#^2 = g @ N_0^* \#^2,$$

where

$$g = k^* t^* - c_0 \bar{w}^2 = k^* t \bar{w}^2 \frac{-c K_0 t^2}{-1 + c K_0 t^3}. \quad -4.11!$$

The maximum of this quantity is reached at $c = 2/(K_0 t)$. In the contact approximation it is

$$g_{\max} = \frac{4}{27} k^* t \bar{w}^2 = t \frac{4}{27} \frac{k_b'}{k_D} \frac{-k_D + k_r}{k_D + k_r + k_b'}. \quad -4.12!$$

According to Eqs. -3.22! and -2.7! we have

$$\begin{aligned} k_r' & w_r v \exp\left(-\frac{(DG_r + l_c)^2}{4l_c T}\right), \\ k_b' & w_b v \exp\left(-\frac{(DG_i - l_c)^2}{4l_c T}\right), \quad k_i \exp(-DG_i/T), \end{aligned} \quad -4.13!$$

where v is the reaction volume and $DG_b = \mathcal{E} + DG_r = -DG_i$. At fast diffusion $g \gg k_b$ reaches maximum at $DG_i = l_c$. At smaller concentrations $@c \ll 2/(K_0 t) \#$ it follows from -4.11! and -4.8! that $g \gg k_b k_i^2$. The maxima of these Gaussians are shifted in opposite directions ($DG_i = \pm l_c$). Hence, $g \gg 0$ only near $DG_i = 0$, where they overlap @Fig. 8-b!#.

In Fig. 9 we showed the kinetics of the excited state decay with and without taking into account the bimolecular reverse transfer in the volume. In the latter case there is a false asymptotic behavior at long times, noticed in Refs. 24

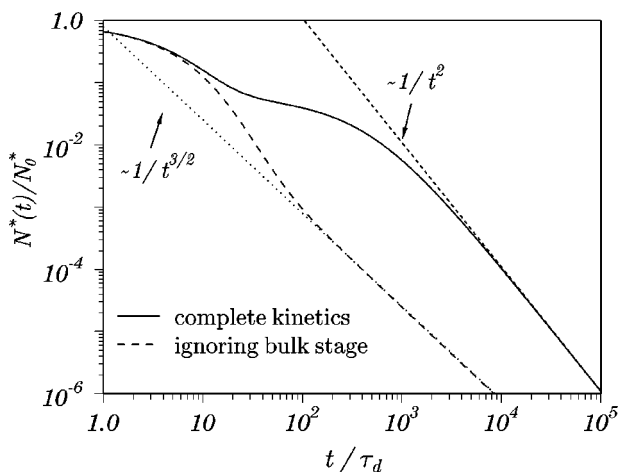
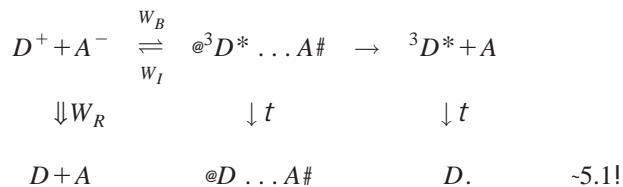


FIG. 9. The false asymptotics of geminate excitation quenching (long dashed line) in comparison to the power asymptotics (dashed line) of true excitation decay (solid line). All parameters are the same as for Fig. 8-a).

and 27: $N^*(t) \sim t^{-3/2}$. This behavior peculiar to IET, even in the complete absence of reverse transfer, can be eliminated using properly modified encounter theory (MET),^{28,29} or an improved superposition approximation.^{27,30} The substitution of MET for IET is inevitable for studying the long-time asymptotics of highly exergonic ionization, which is practically irreversible. However, in the case of reversible ionization the bimolecular pumping of the excited state hinders and turns its decay to a much slower quasistationary evolution (4.7). At strong pumping this may happen before the false asymptotics is reached (Fig. 9). As a result, the whole excitation decay from the very beginning until the end is perfectly described by IET. As shown in Fig. 9, the delayed fluorescence at long times follows the predicted power dependence of time (4.9), which is easy to distinguish from anything else. It differs from either false asymptotics or exponential decay, superseding it in more accurate theories.^{27,28}

V. ELECTROCHEMILUMINESCENCE

The right half of reaction (1.2) can be realized apart from the left half. This can be done by injection of ions, subjected to subsequent recombination to the ground and excited states:



This is the process studied in Refs. 16 and 17 through the luminescence coming from ${}^3D^*$. The quantum yield of excitations, f_{es} , can be extracted from the electrochemiluminescence quantum yield f_{ecl} , if the emission quantum yield from the excited state f_e is known:¹⁶

$$f_{ecl} = f_e f_{es}. \quad (5.2)$$

In Refs. 16 and 17 the f_{es} dependence on the free energy of ionization, $DG_i = -DG_b$, was measured for a number of systems. To specify this dependence we have to calculate

$$f_{es} = \frac{\int_0^\infty N^*(t) dt}{N^+_0 t}, \quad (5.3)$$

borrowing $N^*(t)$ from the solution of Eqs. (2.1) where we set $I_0 = 0$ and use the new initial conditions created by the external injection of ions into solution:

$$N^*_0 = 0, \quad N^+_0 = N_0. \quad (5.4)$$

Making the Laplace transformation of Eq. (2.1) under these conditions and excluding $\int_0^\infty N^+(t) dt$ we obtain

$$\begin{aligned}
 f_{es} &= \tilde{N}^*_0 / N_0 t \\
 &= \frac{1}{\tilde{R}^*_0 / \tilde{R}^\#_0 + c t @ \tilde{R}^*_0 / \tilde{R}^\#_0 / \tilde{R}^\#_0 - \tilde{R}^\dagger_0 / \tilde{R}^\#_0}.
 \end{aligned} \quad (5.5)$$

Since this result is expressed through kernels taken at $s=0$, it does not depend on the spatial dispersion of the initial conditions for the auxiliary functions (see the Appendix). The initial spatial correlations in the system affect only the kinetics of luminescence but not the stationary values that can be obtained from general expressions like Eq. (4.4) setting $s=0$. Such expressions for all the kernels are listed in Ref. 7. Using them we obtain from Eq. (5.5) the contact estimate of the excited state quantum yield:

$$f_{es} = \frac{1}{1 + 1 + c t k_{irr} k_r / k_b}, \quad (5.6)$$

where k_{irr} and k'_b are given by Eqs. (3.33) and (4.5).

In Refs. 16 and 17 the recombination into the excited state was considered as an irreversible reaction. If this is true, then $k_i = 0$ ($k_{irr} = 0$ and $k'_b = k_b$) and general Eq. (5.6) reduces to the simplest one used in these works:

$$f_{es} = \frac{1}{1 + k_r / k_b}. \quad (5.7)$$

With contact estimates of the reaction constants (4.13) we obtain from Eq. (5.7):

$$f_{es} = \frac{1}{1 + w_r / w_i \exp\left(-\frac{\mathcal{E} - DG_i - I_c + \mathcal{E}/2}{2I_c T}\right)}. \quad (5.8)$$

This is a stepwise function which approaches unity with increasing DG_i , because the recombination to the excited state becomes much faster than to the ground state (Fig. 10). It resembles the experimental results obtained in Refs. 16 and 17, although the plateau in these works is usually much lower than 1. This is an indication of the quenching of excited states by survived ions, or through biexcitonic production of singlets and their subsequent decay.

If electron transfer is reversible, the simple expression (5.7) can be obtained from Eq. (5.6), only in the kinetic (fast diffusion) limit: at $k_i \ll k_D = 4\rho S\tilde{D}$. The break on curve (5.8) occurs at $DG_i = I_c - \mathcal{E}/2$, while k_i reaches its maximum at

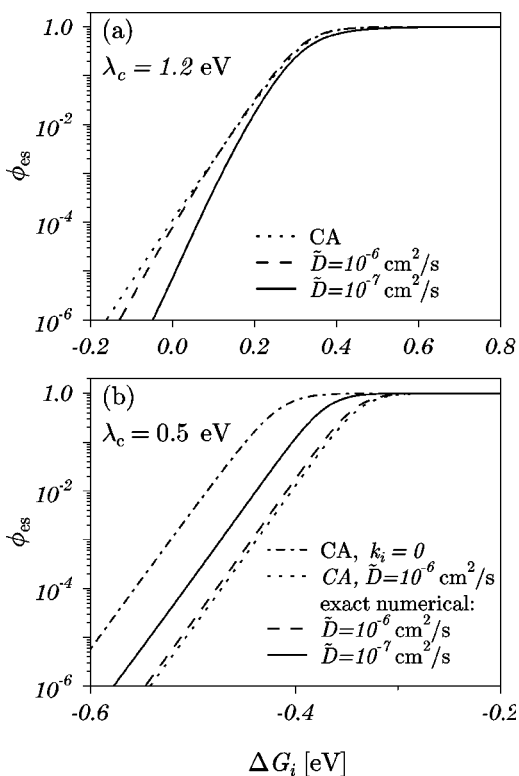


FIG. 10. The quantum yield of excited states as a function of the ionization free energy at large -a! and small -b! reorganization energy of electron transfer λ_c . In these two cases the increase of diffusion from $\bar{D} = 10^{-7}$ cm²/s -solid lines! to $\bar{D} = 10^{-6}$ cm²/s -long dashed lines! shifts the curve in the opposite directions. Contact calculations -CA! of the same curves are made with and without taking into account the reverse electron transfer to ionized state.

$\Delta G_i = -\lambda_c$. Only there it may exceed k_D , changing control from kinetic to diffusional ($k_i \gg k_D$). However, at large λ_c the distance between the break and this points, $dG = 2\lambda_c - \mathcal{E}/2$, is so large that $k_i/k_D \ll 1$ everywhere. At $\lambda_c = 1.2$ eV, k_i is negligible everywhere and the results obtained in the contact approximation from either Eq. -5.6! or -5.7! are the same @the upper curve in Fig. 10-a!#.

Beyond the contact approximation diffusion not only changes the ratio k_i/k_D , but affects also the competition between recombination to the ground and excited states. Since the recombination is more exergonic its reaction layer has a larger radius. The ions approaching each other must cross the recombination layer to reach the excitation one. Slowing down diffusion one can make the recombination so strong that almost all ions will be neutralized in the outer layer and contribute nothing to the excitation. Hence, at slower diffusion the recombination to the ground state is more favorable and the excitation quantum yield is smaller.

This effect is clearly seen in Fig. 10-a!, but almost disappears in Fig. 10-b!. Since recombination at smaller λ_c is more remote and weaker, it is under kinetic control when the contact approximation is perfect. In Fig. 10-b! there is a small difference between this approximation and the exact calculation, but only for the slowest diffusion. At larger \bar{D} the preference of excitation is due to the increase of k_i/k_D , which slows down the recombination to the excited state.

This effect is well described by general contact formula -5.6!.

VI. CONCLUSIONS

The qualitative influence of ionization reversibility on stationary fluorescence was recently described in Ref. 7, by means of integral encounter theory. Here we use the same theory to study the transient effects initiated by either instantaneous photoexcitation of neutral reactants, or electrochemical injection of counterions into solution.

It was found that reverse electron transfer to excited states reduces the quantum yield of their ionization after excitation. This is the case in a narrow free energy region where ionization is quasisonant and under very specific conditions: at slow diffusion and at a small reorganization energy of transfer. The rigidity of these conditions explains why the reverse transfer might be neglected in the vast majority of time-resolved studies of photoionization. However, two other effects studied here in principle cannot be understood without taking into account the reverse transfer. These are delayed fluorescence caused by bimolecular recombination of ions in a bulk and chemiluminescence initiated by recombination of free ions injected into solution. The kinetics of fluorescence and the free energy dependence of its quantum yield were studied with the same set of IET equations as primary photoionization.

It should be stressed that IET is especially appropriate to account for reversible reactions,^{24,10,7} but only in the lowest order approximation with respect to concentration of reactants. To extend the study to higher concentrations or longer asymptotics of geminate recombination, IET should be substituted by MET which accounts for all binary terms of the concentration expansion.²⁹ However, for the present and many other goals, IET provides the simplest, but fundamentally proven method of a new non-Markovian photochemistry.¹² To solve numerically the integrodifferential equations of IET very effective programs were developed and used here. IET incorporated with these programs is actually the universal key to any transfer reactions, provided that their elementary rates, depending on interparticle distance, are borrowed from the appropriate microscopic theory.

ACKNOWLEDGMENTS

This work was supported by the Israel Science Foundation, grant of 6th competition -1999! of RAS young scientists projects -project 151! and RFBR grant of young scientists projects -project 01-03-6300!.

APPENDIX: INITIAL CORRELATIONS OF IONS

We assume that the uniform mixing of ions is accomplished before recombination starts. If they are mixed right up to their equilibrium distribution in a Coulomb well $U(r)$, then their density there is

$$F(r) = \exp[-U(r)/T] \quad \text{-A1!}$$

The kernels of integral equations -2.1a! remain unchanged, except those for ion recombination. The auxiliary differential equations for them are the same,

$$\dot{g} = -W_I r!g + W_B r!f - \frac{1}{t}g + \mathcal{L}_r g, \quad \text{-A2a!}$$

$$\dot{f} = W_I r!g - W_B r!f - W_R r!f + \mathcal{L}_r^c f, \quad \text{-A2b!}$$

but they should be solved with different initial conditions. It is easy to see that Eq. -2.6! is the Laplace transformation of -A2a! and -A2b!, provided $f(r;0) = 1$, $g(r;0) = 0$. These initial conditions reflect the uniform distribution of photogenerated ions. Making the same Laplace transformation now we should take different initial conditions:

$$f-r;0! = F-r!, \quad g-r;0! = 0. \quad \text{-A3!}$$

This difference is due to a different preparation of the system. The free ions produced by separation of different photogenerated pairs are noncorrelated and their distribution in space is homogeneous. On the contrary, the equilibrium distribution established by perfect mixing of injected ions is not homogeneous within Coulomb wells. There is an initial correlation between counterions in those wells.

¹D. Rehm and A. Weller, *Isr. J. Chem.* **8**, 259 -1970!.

²R. A. Marcus and P. Siders, *J. Phys. Chem.* **86**, 622 -1982!.

³T. Kakitani, N. Matsuda, A. Yoshimori, and N. Mataga, *Prog. React. Kinet.* **20**, 347 -1995!; N. Matsuda, T. Kakitani, T. Denda, and N. Mataga, *Chem. Phys.* **190**, 83 -1995!.

⁴I. Z. Steinberg and E. Kachalsky, *J. Chem. Phys.* **48**, 2404 -1968!.

⁵A. B. Doktorov and A. I. Burshtein, *Sov. Phys. JETP* **41**, 671 -1976!.

⁶V. P. Sakun, *Physica A* **90**, 128 -1975!; A. B. Doktorov, *ibid.* **90**, 109 -1978!; A. A. Kipriyanov, A. B. Doktorov, and A. I. Burshtein, *Chem. Phys.* **76**, 149 -1983!.

⁷A. I. Burshtein and K. L. Ivanov, *J. Phys. Chem. A* **105**, 3158 -2001!.

⁸A. A. Kipriyanov, I. V. Gopich, and A. B. Doktorov, *Chem. Phys.* **187**, 241 -1994!; **191**, 101 -1995!.

⁹I. V. Gopich, A. A. Kipriyanov, and A. B. Doktorov, *J. Chem. Phys.* **110**, 10888 -1999!.

¹⁰A. I. Burshtein and N. N. Lukzen, *J. Chem. Phys.* **103**, 9631 -1995!; **105**, 9588 -1996!.

¹¹A. I. Burshtein and P. A. Frantsuzov, *J. Chem. Phys.* **106**, 3948 -1997!.

¹²A. I. Burshtein, *J. Lumin.* **93**, 229 -2001!.

¹³K. Zachariasse, Ph.D. thesis, Free University, Amsterdam, 1972.

¹⁴A. Weller and K. Zachariasse, in *Chemiluminescence and Bioluminescence*, edited by M. J. Cormier, D. M. Hercules, and J. Lee -Plenum, New York, 1973!, p. 169.

¹⁵K. Zachariasse, in *The Exciplex*, edited by M. Gordon and W. R. Ware -Academic, New York, 1975!, p. 275.

¹⁶R. D. Mussell and D. Nocera, *J. Am. Chem. Soc.* **110**, 2764 -1988!; *Inorg. Chem.* **29**, 3711 -1990!.

¹⁷P. Szrebrowaty and A. Kapturkiewicz, *Chem. Phys. Lett.* **328**, 160 -2000!.

¹⁸S. S. Jayanthi and P. Ramamurthy, *J. Phys. Chem. A* **101**, 2016 -1997!; **102**, 511 -1998!; *PCCP* **1**, 4751 -1999!.

¹⁹A. I. Burshtein, *Adv. Chem. Phys.* **114**, 419 -2000!.

²⁰O. A. Igoshin and A. I. Burshtein, *J. Chem. Phys.* **112**, 10930 -2000!; *J. Lumin.* **92**, 123 -2000!.

²¹N. N. Lukzen, E. B. Krissinel, O. A. Igoshin, and A. I. Burshtein, *J. Phys. Chem.* **105**, 19 -2001!.

²²A. I. Burshtein, I. V. Gopich, and P. A. Frantsuzov, *Chem. Phys. Lett.* **289**, 60 -1998!.

²³A. I. Burshtein, A. A. Zharikov, N. V. Shokhirev, O. B. Spirina, and E. B. Krissinel, *J. Chem. Phys.* **95**, 8013 -1991!.

²⁴N. N. Lukzen, A. B. Doktorov, and A. I. Burshtein, *Chem. Phys.* **102**, 289 -1986!.

²⁵A. I. Burshtein and E. B. Krissinel, *J. Phys. Chem.* **100**, 3005 -1996!.

²⁶A. I. Burshtein, *Chem. Phys. Lett.* **194**, 247 -1992!.

²⁷J. Sung, J. Chi, and S. Lee, *J. Chem. Phys.* **111**, 804 -1999!.

²⁸I. V. Gopich, A. A. Kipriyanov, and A. B. Doktorov, *J. Chem. Phys.* **110**, 10888 -1999!.

²⁹K. L. Ivanov, N. N. Lukzen, A. B. Doktorov, and A. I. Burshtein, *J. Chem. Phys.* **114**, 1754 -2001!; **114**, 1763 -2001!.

³⁰J. Sung and S. Lee, *J. Chem. Phys.* **112**, 2128 -2000!.